**LA-UR-25-23464**
**Accepted Manuscript**

# Ultrafast laser triggered electron emission from ultrananocrystalline diamond pyramid tip cathode

Kachwala, Ali
Chubenko, Oksana
Kim, Dongsung
Simakov, Evgenya Ivanovna
Karkare, Siddarth

Provided by the author(s) and the Los Alamos National Laboratory (2025-04-10).

**To be published in:** Journal of Applied Physics

**DOI to publisher's version:** 10.1063/5.0196457

**Permalink to record:**
https://permalink.lanl.gov/object/view?what=info:lanl-repo/lareport/LA-UR-25-23464

Los Alamos National Laboratory, an affirmative action/equal opportunity employer, is operated by Triad National Security, LLC for the National Nuclear Security Administration of U.S. Department of Energy under contract 89233218CNA000001. By approving this article, the publisher recognizes that the U.S. Government retains nonexclusive, royalty-free license to publish or reproduce the published form of this contribution, or to allow others to do so, for U.S. Government purposes. Los Alamos National Laboratory requests that the publisher identify this article as work performed under the auspices of the U.S. Department of Energy. Los Alamos National Laboratory strongly supports academic freedom and a researcher's right to publish; as an institution, however, the Laboratory does not endorse the viewpoint of a publication or guarantee its technical correctness.

Journal of Applied Physics

RESEARCH ARTICLE | MARCH 27 2024

# Ultrafast laser triggered electron emission from ultrananocrystalline diamond pyramid tip cathode

A. Kachwala ; O. Chubenko ; D. Kim ; E. I. Simakov ; S. Karkare

Check for updates

*J. Appl. Phys.* 135, 124902 (2024)
https://doi.org/10.1063/5.0196457
CHORUS

View Online
Export Citation

## Articles You May Be Interested In

Quantum efficiency, photoemission energy spectra, and mean transverse energy of ultrananocrystalline diamond photocathode

*J. Appl. Phys.* (December 2022)

Cryogenic operation of planar ultrananocrystalline diamond field emission source in SRF injector

*Appl. Phys. Lett.* (February 2021)

Theoretical evaluation of electronic density-of-states and transport effects on field emission from n -type ultrananocrystalline diamond films

*J. Appl. Phys.* (May 2019)

10 April 2025 23:03:47

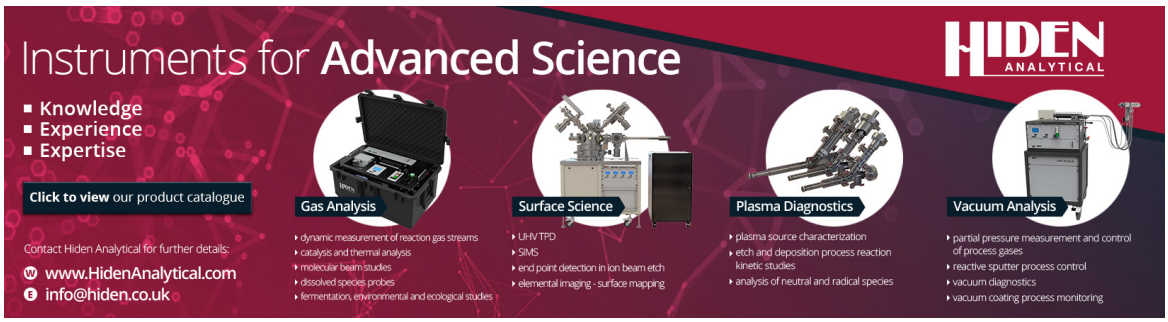


AIP Publishing

Journal of Applied Physics ARTICLE pubs.aip.org/aip/jap

# Ultrafast laser triggered electron emission from ultrananocrystalline diamond pyramid tip cathode

Cite as: J. Appl. Phys. **135**, 124902 (2024); doi: 10.1063/5.0196457
Submitted: 7 January 2024 · Accepted: 6 March 2024 ·
Published Online: 27 March 2024

View Online Export Citation CrossMark

A. Kachwala,[1,a)] O. Chubenko,[2] D. Kim,[3] E. I. Simakov,[3] and S. Karkare[1,a)]

## AFFILIATIONS

[1]Department of Physics, Arizona State University, Tempe, Arizona 85287, USA
[2]Department of Physics, Northern Illinois University, DeKalb, Illinois 60115, USA
[3]Accelerator Operations and Technology Division, Los Alamos National Laboratory, Los Alamos, New Mexico 87545, USA

[a)]**Authors to whom correspondence should be addressed:** akachwal@asu.edu and karkare@asu.edu

## ABSTRACT

Nitrogen-incorporated ultrananocrystalline diamond [(N)UNCD] pyramid tip cathode has been considered as a next-generation high peak current electron source for dielectric laser accelerators as well as other high peak current particle accelerator applications. In this work, we study non-linear photoemission from an (N)UNCD pyramid tip cathode using an ultrafast laser with the pulse length of 150 fs with the central wavelength of 800 nm in the peak intensity range of $10^9$–$10^{10}$ W/cm$^2$. We demonstrated that as the incident laser intensity increases, the current emitted from the nano-tip first increases as a power function with an exponent of about 5 and then starts to roll over to an exponent of 3. This roll over is attributed to the Coulomb interaction between electrons emitted from the tip also known as the space charge. We also measured the photoemission electron energy spectra that show electrons with energies as high as ∼10 eV. Based on the shape of the electron energy spectra, we conclude that the high-energy electrons are thermally emitted electrons due to ultrafast laser heating at the tip of the (N)UNCD pyramid tip cathode.

10 April 2025 23:03:47

*© 2024 Author(s). All article content, except where otherwise noted, is licensed under a Creative Commons Attribution (CC BY) license (https://creativecommons.org/licenses/by/4.0/).* https://doi.org/10.1063/5.0196457

## I. INTRODUCTION

The widespread use of particle accelerators for basic research,[1] ultrafast electron diffraction and microscopy,[2] as well as medicine[3] calls for the need to develop compact accelerators with table top dimensions. A novel approach for downsizing particle accelerators and achieving higher acceleration gradient involves utilizing the interaction between charged particles and laser fields. Several techniques fall under this category, including laser-wakefield acceleration,[4–6] direct laser acceleration through the longitudinal component of radially focused laser light,[7] and dielectric laser acceleration (DLA).[8,9] Dielectric and semiconductor materials have damage thresholds that correspond to acceleration fields in the range of 1–10 GV/m,[10,11] significantly higher than those in conventional metallic cavity-based accelerators.[12] DLAs are microstructures made of dielectric materials powered by lasers with wavelengths between 800 nm and 2 $\mu$m.[13,14] Recent experiments have demonstrated the acceleration of relativistic electrons using dielectric grating microstructures, achieving accelerating gradients of 690 MV/m, which is ten times greater than traditional metallic cavity-based accelerators.[15] It is believed that the DLA can achieve the accelerating gradient of as high as ∼1 GV/m, which would enable the development of next-generation compact accelerators.

A critical element of any particle accelerator, including the DLA, is the electron source known as the cathode. Due to the compact nature of the DLA's transverse structure, typically ranging a few micrometers, there is a demand for exceptionally small, high-current density electron sources that can be triggered by a laser. This laser-triggered photoemission simplifies the challenges associated with synchronizing the electron beam and the acceleration system. In addition, a DLA also requires a source with low emittance (sub-100 nm-rad), guaranteeing small divergence of the beam along the path of acceleration.[13]

Ultrananocrystalline diamond (UNCD) is a promising candidate for such applications because of its mechanical and electrical stability along with an intrinsically fast response time (∼100 fs).[16,17] Moreover, its vacuum robustness makes it a promising candidate for DLA and other high peak current accelerator applications. To improve the photoemission performance of UNCD and thereby extract more current, negative electron affinity (NEA) of the


© Author(s) 2024

diamond can be exploited. A way to do so would be by *n*-doping of the UNCD and surface treatment in a hydrogen environment.[18] Recently, *n*-doping of micro-, nano-, and ultrananocrystalline diamond films using nitrogen has been performed by many groups.[19–21] In UNCDs, the nitrogen predominantly enters the grain boundaries and does not form trapped states within the diamond gap. It has been shown that the addition of nitrogen to UNCD films increases its electrical conductivity upto 1854 S cm$^{-1}$ and the maximum current density to 8 mA cm$^{-2}$.[22] This is advantageous for DLA as well as other high peak current accelerator applications. Such films with nitrogen incorporation are termed as nitrogen-incorporated ultrananocrystalline diamond (N)UNCD.

Another advantage of (N)UNCD is that it can be molded into a pre-defined shape, even at nano-scale. To meet the transverse dimension, current density, and emittance requirements of DLA, (N)UNCD can be molded into micrometer-scale diamond pyramid with sharp tip at the apex.[23] These (N)UNCD pyramid tip cathodes (PTCs) can be triggered by a laser to simplify the issues of synchronization of the electron beam and the accelerating structure. When used in the non-linear photoemission regime with infra-red light, the sharp tip at the apex can enhance the optical electric field of the incident laser, thereby resulting in nanometer-scale emission area, and, hence, achieve sub-micrometer-scale normalized transverse emittance. These photoemission properties make the (N)UNCD PTC a promising candidate for DLA applications. In addition, the (N)UNCD PTC can also be used for electron microscopy, nanoelectronics, as well as high-peak current accelerator applications.

The field emission studies of (N)UNCD PTC have been performed by many groups.[24–29] In the field emission mode, using (N)UNCD PTC, the maximum single tip current measured was as high as 18 $\mu$A.[30] Furthermore, (N)UNCD PTCs have demonstrated an effective emission area of 400 nm$^2$ with an average emission current as high as 2 $\mu$A.[27] However, in order to have sub-picosecond electron bunch lengths required for DLA as well as other particle accelerator applications, the (N)UNCD PTC needs to be operated in the photoemission regime. The linear photoemission mechanism, where the operating photon energy is higher than or at the work function of the (N)UNCD, as well as (N)UNCD PTC is very well understood and performed by many groups.[31–35]

In order to have a nanometer-scale emission area from (N)UNCD PTC, they need to be operated in the non-linear photoemission regime. Operating in non-linear photoemission regime results in the optical field enhancement at the tip of (N)UNCD PTC and thereby result in electron emission only from the nanometer scale tip of the cathode. Non-linear photoemission studies from (N)UNCD PTC using infrared wavelengths have been performed by two groups.[35,36] Both of them observe the characteristic change in non-linearity in electron count with increasing laser intensity. However, the mechanism responsible for this change in non-linearity is not very well understood. In certain studies, the non-linear photoemission measurements were done for (N)UNCD PTC at different infrared wavelengths ranging from 800 to 2000 nm with peak laser intensities in the range of $10^9$–$10^{10}$ W/cm$^2$.[35,36] At each of these wavelengths, a characteristic change in non-linearity in electron count rate with increasing laser intensity was observed. They also observed increase in electron emission spot size at high laser intensities. As a result, the change in non-linearity was attributed to Coulomb interaction between electrons emitted from the (N)UNCD PTC or the space charge. In another study, the change in non-linearity was attributed to the strong field photoemission from (N)UNCD PTC.[37] In strong field photoemission, the emitted electron can re-scatter with the parent photocathode under the influence of the electric field of the laser. These re-scattered electrons can have trajectories that can result in increase in the electron emission spot size. However, none of these studies measured the kinetic energy distribution of the emitted electrons that would explain the change in non-linearity and thereby aid in understanding the emission mechanism from (N)UNCD PTC.

In this work, we report the measurements of scaling of the electron count rate with incident laser intensity and photoemission electron energy spectra (PEES) in the non-linear photoemission regime from (N)UNCD PTC using a photoemission electron microscope (PEEM). The change in non-linearity was observed with increasing laser intensity, which was consistent with the previously reported data. However, at low intensity regime, we observe 5th-order photoemission process as opposed to 8th–12th order observed for previous works. We attribute this 5th-order photoemission process to above-threshold photoemission (ATP) that is regularly observed for needle-tip photocathodes or to the emission from direct bandgap of diamond. At high laser intensities, we observe the *kink* resulting in the change in non-linearity from 5 to 3. We also observe increase in electron emission spot size beyond the *kink*. To further understand the emission mechanism, we measured the PEES that shows electron with energies as high as ~10 eV. Based on the shape of the PEES, we conclude that the high-energy electrons are not emitted due to strong field photoemission but instead are thermally emitted electrons due to laser heating at the tip of (N)UNCD PTC and the increase in spot size is attributed to the Coulomb interaction between electrons emitted from the (N)UNCD PTC.

10 April 2025 23:03:47

## II. EXPERIMENTAL DETAILS

### A. Sample preparation

The diamond deposition process for the synthesis of (N)UNCD films was performed by Advanced Diamond Technologies. Details of different steps for the preparation of (N)UNCD are reported elsewhere.[23] Typically, it has 1 $\mu$m layer of conductive (N)UNCD film, followed by a layer of 15 $\mu$m microcrystalline diamond. Diamond film is brazed to a polished Mo substrate using the brazing material TiCuSil.

Figure 1(a) shows the Raman spectrum of an (N)UNCD sample. The broad peaks at 1350 and 1550 cm$^{-1}$ correspond to the characteristic disordered diamond (D) peak and graphite (G) peak, respectively. Figures 1(b) and 1(c) show the scanning electron microscope image (SEM) of (N)UNCD PTC. As shown in Fig. 1(b), the pyramid has a base of ~25 $\mu m$ with the aspect ratio of 0.7. Figure 1(c) shows a sharp emitter tip at the apex of the pyramid. The radius of the tip was ~15 nm.

### B. Measurement details

The schematic of the experimental setup is shown in Fig. 2. The measurements were performed using a 500 kHz repetition rate


© Author(s) 2024

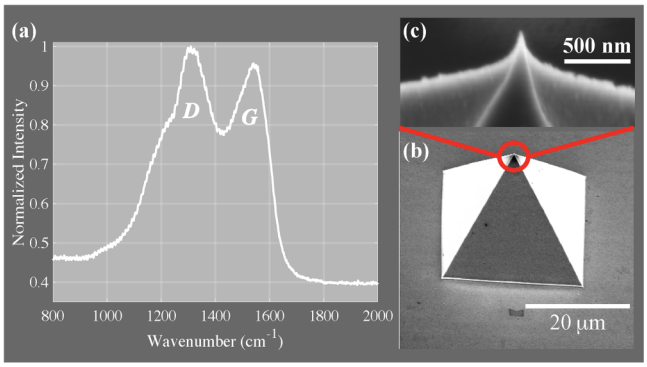


**FIG. 1.** (a) Raman spectrum of the (N)UNCD sample showing a characteristic disordered diamond (D) peak and graphite (G) peak. Scanning electron microscope (SEM) image of (b) (N)UNCD PTC and (c) sharp tip with radius ∼15 nm at the apex of (N)UNCD PTC.

femtosecond pulsed laser with a pulse length of 150 fs from a pulsed Optical Parametric Amplifier (Light Conversion Orpheus pumped by Light Conversion Pharos) and central wavelength of 800 nm. The laser was made incident onto the sample at 65° angle of incidence with respect to the axis of the (N)UNCD PTC and was focused by a lens down to the spot size of $80 \times 150\,\mu m^2$. The polarization of the electric field is shown in Fig. 2, and all the measurements were performed in this mode (p-polarized on the sample) of laser polarization. One-millimeter real space field of view (significantly larger than the laser spot size) was selected to image all the photoemitted electrons using a double micro-channel plate (MCP) detector at the end of a commercially available PEEM column from Focus gmbh.[38] The number of electrons emitted from the tip was determined by recording counts/second on the MCP detector and using a predetermined calibration factor to convert it into electrons per shot at different values of incident laser intensities.

The photoemission spectra were obtained by using the imaging energy filter (IEF) capability of the PEEM. Background subtracted energy-filtered images were obtained for the (N)UNCD PTC sample with ∼100 meV energy resolution. The contrast aperture (CA) of a 1750 $\mu$m diameter placed in the backfocal plane of the objective lens in the PEEM column was selected to ensure transmission of all the emitted electrons from the surface of the sample. After acquiring the energy-filtered images, a numerical differentiation of high pass energy spectrum was performed and the normalized counts were plotted against the kinetic energy of emitted electrons for different incident laser intensities. A detailed description of the measurement procedure can be found in Ref. 34. An electric field bias of 5 kV/m was applied between the cathode and the extractor of the PEEM. The bias was low enough so that there was no observed dark current in the absence of the incident laser. Reliable spatial and *k*-space images could not be obtained due to the pyramids distorting the accelerating fields in the PEEM.

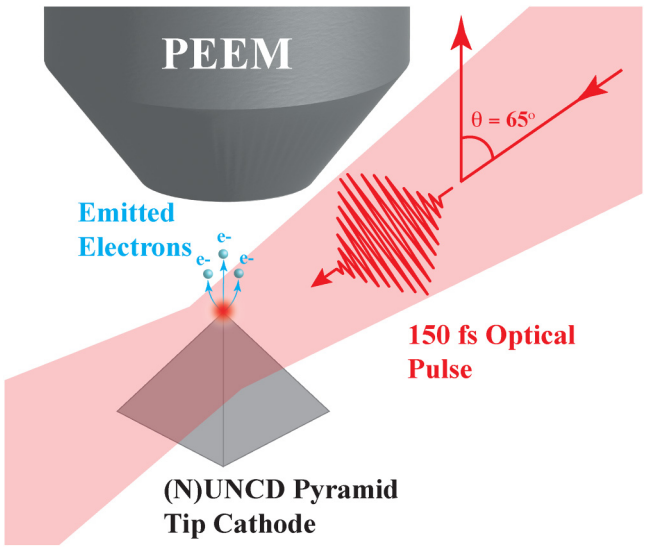


**FIG. 2.** Schematic of experimental setup showing (N)UNCD PTC illuminated by femtosecond laser with the pulse length of 150 fs and central wavelength of 800 nm. The laser was made incident onto the sample at 65° with respect to the axis of (N)UNCD PTC. The sharp tip at the apex of (N)UNCD PTC results in field enhancement of the incident laser field. The electron emitted from the sharp tip at the apex of (N)UNCD pyramid is imaged using the photoemission electron microscope (PEEM).

## III. RESULTS AND DISCUSSION

Figure 3 shows the results of our measurements of the number of electrons emitted per shot from the (N)UNCD PTC

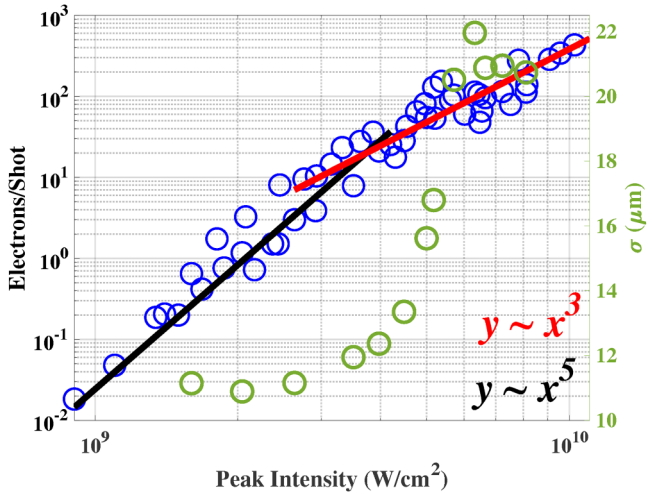


**FIG. 3.** Logarithmic representation of electrons per shot (in blue) emitted from (N)UNCD PTC as the function of peak laser intensity. Semi-logarithmic representation of evolution of root mean square spot size (in green) of electrons detected on the micro-channel plate detector of the PEEM plotted as a function of peak laser intensity.

10 April 2025 23:03:47


© Author(s) 2024

plotted as a function of peak laser intensity on a double logarithmic scale. For the same value of peak laser intensity, the number of electrons emitted per shot from the (N)UNCD PTC was an order of magnitude higher than the corresponding emission from the (N)UNCD flat substrate.[34] This indicates that the enhancement of optical field is taking place at the tip of the (N)UNCD PTC and that results in more electrons being emitted per shot for the same range of peak laser intensity when compared to the (N)UNCD substrate. Considering the work function ($\Phi$) of (N)UNCD to be ~4.4 eV,[34] using 1.55 eV photon energy should result in third-order photoemission. However, for the case of (N)UNCD PTC, at the peak intensities less than ~4 GW/cm$^2$, the exponent of the peak intensity dependence suggests a fifth-order photoemission process. The 5th order of non-linearity that is quite different from the 8th–12th orders observed in previous studies[35,36] could be due to the different curvatures of the (N) UNCD PTC as well as different doping concentrations. Other than the tip shape and doping, the angle of incidence and the polarization of the laser may also play a role. Previous studies have reported the angle of incidence to be 84°, whereas we have a 65° angle of incidence. The angle of incidence could also make a difference in the order of emission from (N)UNCD PTC. In general, the lowest multiphoton order $n_{min}$ dominates the photoemission rate in the multiphoton regime. However, at higher value of laser intensity, there is substantial contributions from higher multiphoton orders $n > n_{min}$. This emission mechanism is called above-threshold photoemission (ATP).[39,40] The fifth-order photoemission process could be a result of ATP. The fifth-order photoemission process could also be a result of electron emission from the direct bandgap of diamond.[41] Electrons can be excited into the conduction band across the direct bandgap (7.1 eV[41]) of diamond. These electrons can migrate to the surface and emit into the vacuum. Using 1.55 eV photon energy, fifth-order photoemission process would correspond to ~7.7 eV of photon energy being absorbed by the electrons, which is above the photoemission threshold of emission from the direct bandgap of diamond. A similar higher order photoemission mechanism has been observed from nanocrystalline diamond-coated tungsten tips and was attributed to the electron emission from the direct bandgap of diamond.[42]

At ~4 GW/cm$^2$, a soft *kink* followed by a change of slope in electrons per shot vs peak laser intensity plot is observed. This *kink* results in the change in non-linearity from 5 to 3. The transition from multiphoton electron emission to strong field photoemission is marked by a similar characteristic change in nonlinearity.[40] The change of slope could also occur due to the Coulomb interaction between electrons emitted from the photocathode and screening of the electric field by the electron cloud also known as space charge or due to filling of the excited states prohibiting excitation.

To further elucidate this change in non-linearity, we measured the electron emission spot size measured on the MCP detector at the end of the PEEM column as the function of peak laser intensity. This root mean square electron emission spot size as a function of peak laser intensity is shown on a semi-log plot in Fig. 3. We can see that with the increase in peak laser intensity, the electron emission spot size increases. A similar behavior was also observed in Ref. 36. Owing to this observation, at first glance, it appears that the change in non-linearity is due to the Coulomb interaction between electrons emitted from the photocathode and screening of the electric field by the electron cloud. However, in strong field photoemission, the re-scattered electrons can have trajectories that can result in the increase in the electron emission spot size.

One way to understand whether the electron emission is due to strong field photoemission is by measuring the kinetic energy spectra of the emitted electrons. For the case of strong field emission, the local laser electric field steers the motion of a photoemitted electron and can cause the electron to return to the parent photocathode. The photoelectron then eventually scatters with the parent photocathode and recollision takes place. This is clearly observed in the electron kinetic energy spectra. The low kinetic energy spectrum is dominated by the direct electrons where the emitted electrons do not return back to the parent photocathode under the influence of strong laser field. This low energy part of the spectrum shows strong exponential decay of the electron count rate with increasing kinetic energy. At higher kinetic energy, the electron count rate does not change with the increasing kinetic energy and a plateau is observed in the electron kinetic energy spectra. The extent of this plateau region on the kinetic energy scale increases with the increase in laser intensity. For the case of tungsten metal tip, with the radius of about 8 nm, this plateau region is observed in the electron kinetic energy range of 5–12 eV for the peak intensity range of $0.55 \times 10^{11}$ to $1.3 \times 10^{11}$ W/cm$^2$.[40] At even higher kinetic energies, the count rate again drops dramatically. The energy position where this strong decay starts is called cut-off. Plateau and cut-off are formed by rescattered electrons. If there is a strong field emission from (N)UNCD PTC, we should see the evidence of direct and rescattered electrons in the kinetic energy spectra.

10 April 2025 23:03:47

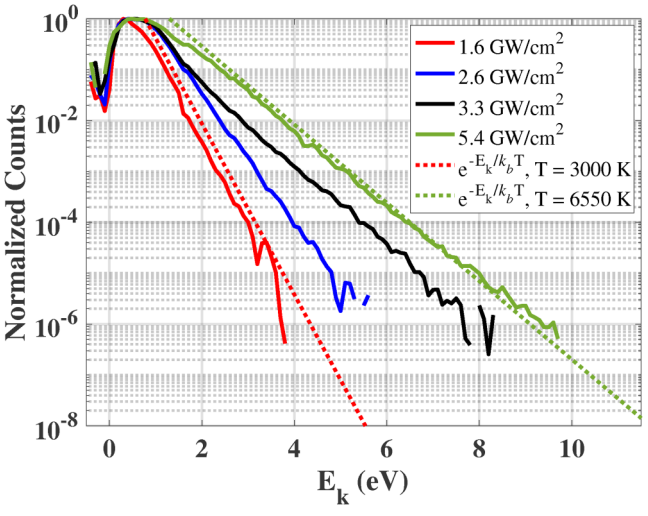


**FIG. 4.** Photoemission electron energy spectra (PEES) at different incident peak laser intensities. The solid lines are the PEES spectra from (N)UNCD PTC. The dotted line is the plot of $e^{-E_k/k_bT}$ with T = 3000 K (red) and T = 6550 K (green). The plot of $e^{-E_k/k_bT}$ was shifted by a constant factor to align with the experimental energy spectrum.


© Author(s) 2024

Figure 4 shows the semi-logarithmic plot of the normalized electron count rate plotted against the kinetic energy of the emitted electrons. From Fig. 4, we see that the kinetic energy spectrum broadens with increasing peak laser intensity. For the case of the fifth-order multiphoton emission process from (N)UNCD PTC, the maximum kinetic energy that the electrons can have is (5 × 1.55 eV) - Φ = 3.4 eV, where Φ = 4.4 eV. Even if we consider the electron emission from the direct bandgap of diamond (7.1 eV[41]), the kinetic energy spread of the emitted electrons should be ∼0.6 eV. However, we see electrons with energies as high as ∼10 eV. In the kinetic energy spectra, we do not observe any plateau or cut-off that appears due to re-scattered electrons, which is the characteristic feature of any strong field photoemission process.

The strong field photoemission regime is characterized using Keldysh theory[43] and is characterized in terms of the Keldysh parameter $\gamma$, which is given by the following equation:

$$\gamma = \sqrt{\frac{\Phi}{2U_p}}, \tag{1}$$

where Φ is the work function and the ponderomotive energy $U_p$ is given by the following equation:

$$U_p = \frac{e^2\alpha^2 {E_0}^2}{4m\omega^2}, \tag{2}$$

where $e$ is the electron charge, $m$ is the mass of the electron, $\alpha$ is the field enhancement factor, $E_0$ is the field strength, and $\omega$ is the angular frequency of the incident light. The strong field photoemission regime is governed by $\gamma << 1$.

To get the estimate of field enhancement at the (N)UNCD PTC, we performed a lumerical FDTD simulation.[44] The geometry of the tip was similar to the (N)UNCD tip used for experiment with the tip radius of 15 nm. A gaussian pulse with a pulse length of 150 fs and a central wavelength of 800 nm was made incident at an angle of 65° with respect to the axis of the (N)UNCD PTC. The refractive index parameters were taken from Ref. 45.

Figure 5 shows field enhancement factor of $\alpha \sim 3$ (which is typical for semiconductor tip of the dimensions similar to (N)UNCD PTC used in this study[46]). Using Eq. (2), a maximum peak laser intensity of 5.4 GW/cm$^2$ and $\alpha = 3$ would result in ponderomotive energy of ∼0.3 μeV. Taking Φ = 4.4 eV, this would result in $\gamma \sim 3900$ that is nearly four orders of magnitude higher than the value of $\gamma$ where strong field photoemission is expected to be observed.

When operating photocathodes with ultrafast (∼100 fs) laser pulses and very large laser intensities (∼GW/cm$^2$), the temperature of electronic distribution is effectively isolated from the lattice and as a result can increase to several thousands of Kelvin.[47,48] This is in part due to large difference in electron and lattice heat capacities. These laser-excited electrons scatter with other non-excited electrons repeatedly, eventually transferring all the laser energy into the thermal energy of electrons, thus heating them. This occurs at sub to few picosecond time scales. As a result, the thermalized electron emission occurs which is not prompt and long tails of high energy electrons are present in the kinetic energy spectra of emitted

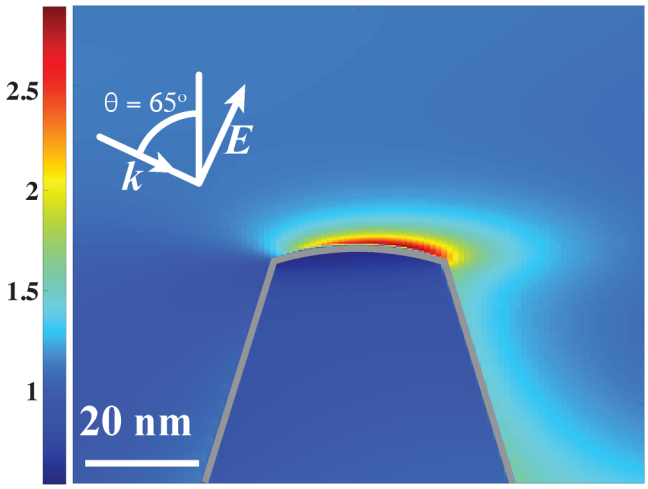


**FIG. 5.** Time average of the optical electric field in vicinity of a sharp (N)UNCD PTC calculated using the lumerical FDTD method. The color encodes the ratio of the local field average and the amplitude of the incident light. The field is enhanced at the surface of the apex by a factor of up to ∼3.

electrons. Such long tails of high energy electrons are present in the kinetic energy spectra shown in Fig. 4. Such thermalized electron emission has also been reported previously for carbon nanotube-based nanotip[49] as well as silver nanotip when operated with a high repetition rate laser.[50] For laser intensity of 1.6 and 5.4 GW/cm$^2$, electron temperature as high as 3000 and 6550 K is reached, respectively. Such high electron temperatures in photoemission have also been reported previously from copper,[51] silver nanotips,[50] tungsten,[52] and carbon nanotube-based nanotip.[49]

After this initial rise in electron temperature, the equilibrium between electron and lattice is reached via electron–phonon scattering and can happen over pico-seconds to tens of picosecond time scale.[51] Diamond possesses the highest thermal conductivity of ∼2000 W/mK in all bulk materials (5 times the thermal conductivity of the best metals such as copper), owing to low phonon scattering in diamond.[53] Since phonon scattering is drastically enhanced by grain boundaries, the thermal conductivity of polycrystalline diamond films is strongly dependent on the grain size. The grain size of UNCD films is of the order of less than 10 nm.[29,54,55] As a result, this significantly reduces the thermal conductivity of UNCD films. The thermal conductivity of UNCD films is reported to be ∼16 W/mK and decreases to ∼8 W/mK with the addition of nitrogen into the film.[56] Such poor thermal conductivity can significantly heat up (N)UNCD PTC lattice during the equilibrium process between the electrons and lattice over pico-seconds to tens of picosecond time scale via electron–phonon scattering. As a result, after thermalization of electron gas and lattice via electron–phonon and phonon–phonon scattering, a steady-state lattice temperature is reached, which can be significantly higher than the room temperature. As a result, this can alter the shape of the tip of the (N)UNCD PTC due to heating process. Such a change in shape was clearly visible in the SEM of the tip performed after the photoemission experiments as shown in Fig. 6(a). The sharp protrusions on the tip

10 April 2025 23:03:47


© Author(s) 2024

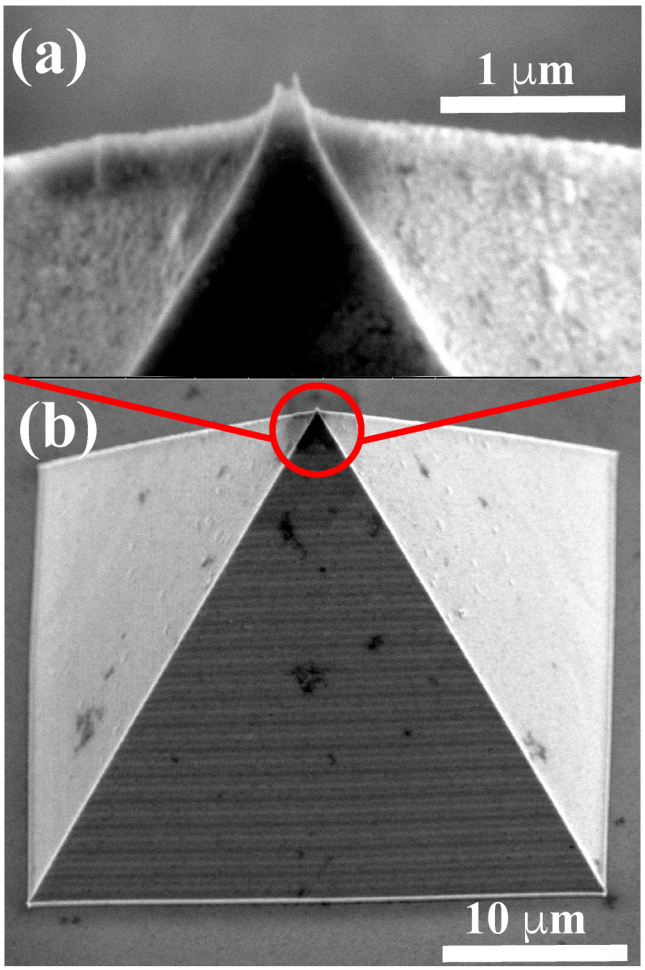


**FIG. 6.** (a) Structural change in the tip at the apex of (N)UNCD PTC after irradiation with femtosecond laser with the pulse length of 150 fs and central wavelength of 800 nm (b) (N)UNCD PTC showing laser-induced periodic surface structures (LIPSS) on the pyramid face exposed to the incident laser. The LIPSS were oriented perpendicular to the direction of the electric field of the incident laser with a spatial period of the order of ∼800 nm.

can also be due to the carbon contamination present inside the SEM, which cannot be discriminated from the diamond.

In addition, from Fig. 6(b), we see that the pyramid face where the laser was incident shows coherent surface structuring after laser irradiation. Such coherent surface structuring was not present before laser irradiation. Such laser-induced periodic surface structures (LIPSS) have been reported on many materials including metals as well as semiconductors after ultrafast laser irradiation.[57–59] These LIPSS are oriented perpendicular to the direction of the electric field of the incident laser with spatial period of the order of wavelength of the incident radiation. LIPSS spaced on the order of wavelength and oriented perpendicular to the direction of the electric field of the incident laser were also observed for (N)UNCD PTC. Such LIPSS for (N)UNCD PTC have also been reported previously after irradiation with femtosecond laser.[35]

## IV. SUMMARY AND CONCLUSION

We measured the scaling of the electron count rate with incident laser intensity and the PEES in the non-linear photoemission regime from (N)UNCD PTC. The measurements were performed with peak laser intensities in the range of $10^9$–$10^{10}$ W/cm$^2$. At low intensity regime, we observe fifth-order photoemission process. We attribute this fifth-order photoemission process to ATP or emission from the direct band gap of diamond. At high laser intensities, we observe the *kink* resulting in the change in non-linearity from 5 to 3. We also observe increase in electron emission spot size beyond the *kink*. We attribute this increase in spot size to Coulomb interaction between electrons emitted from the (N)UNCD PTC. We also measured the PEES that shows electron emitted with kinetic energies as high as ∼10 eV. Based on the shape of the PEES, we conclude that the high-energy electrons are not emitted due to strong field photoemission but instead are thermally emitted electrons due to laser heating at the tip of (N)UNCD PTC.

## ACKNOWLEDGMENTS

This work was supported by the NSF Center for Bright Beams under Award No. PHY-1549132, the DOE under Grant No. DE-SC0021092, and the support of the Los Alamos National Laboratory (LANL) Laboratory Directed Research and Development (LDRD) Program. This work was performed, in part, at the Center for Integrated Nanotechnologies, an Office of Science User Facility operated for the U.S. Department of Energy (DOE) Office of Science. Los Alamos National Laboratory, an affirmative action equal opportunity employer, is managed by Triad National Security, LLC for the U.S. Department of Energy's NNSA, under Contract No. 89233218CNA000001.

10 April 2025 23:03:47

## AUTHOR DECLARATIONS

### Conflict of Interest

The authors have no conflicts to disclose.

### Author Contributions

**A. Kachwala:** Conceptualization (supporting); Data curation (lead); Formal analysis (lead); Investigation (equal); Methodology (equal); Project administration (supporting); Resources (equal); Software (equal); Validation (lead); Visualization (lead); Writing – original draft (lead); Writing – review & editing (supporting). **O. Chubenko:** Conceptualization (supporting); Data curation (supporting); Formal analysis (supporting); Investigation (equal); Methodology (equal); Project administration (supporting); Resources (equal); Software (equal); Validation (supporting); Visualization (supporting); Writing – review & editing (supporting). **D. Kim:** Conceptualization (supporting); Data curation (supporting); Formal analysis (supporting); Investigation (equal); Methodology (equal); Project administration (supporting); Resources (equal); Software (equal); Validation (supporting); Visualization (supporting); Writing – review & editing


© Author(s) 2024

(supporting). **E. Simakov:** Conceptualization (supporting); Data curation (supporting); Formal analysis (supporting); Funding acquisition (supporting); Investigation (equal); Methodology (equal); Project administration (supporting); Resources (equal); Software (equal); Supervision (supporting); Validation (supporting); Visualization (supporting); Writing – review & editing (supporting). **S. Karkare:** Conceptualization (lead); Data curation (supporting); Formal analysis (supporting); Funding acquisition (lead); Investigation (equal); Methodology (equal); Project administration (lead); Resources (equal); Software (equal); Supervision (lead); Validation (supporting); Visualization (supporting); Writing – review & editing (lead).

## DATA AVAILABILITY

The data that support the findings of this study are available from the corresponding authors upon reasonable request.

## REFERENCES


[1]U. Amaldi, "The importance of particle accelerators," Europhys. News **31**, 5–9 (2000).
[2]H. W. Kim, N. A. Vinokurov, I. H. Baek, K. Y. Oang, M. H. Kim, Y. C. Kim, K.-H. Jang, K. Lee, S. H. Park, S. Park *et al.*, "Towards jitter-free ultrafast electron diffraction technology," Nat. Photonics **14**, 245–249 (2020).
[3]M. Silari, "Applications of particle accelerators in medicine," Radiat. Prot. Dosim. **146**, 440–450 (2011).
[4]P. Sprangle, G. Joyce, E. Esarey, and A. Ting, "Laser wakefield acceleration and relativistic optical guiding," AIP Conf. Proc. **175**, 231–239 (1988).
[5]F. Amiranoff, S. Baton, D. Bernard, B. Cros, D. Descamps, F. Dorchies, F. Jacquet, V. Malka, J. Marques, G. Matthieussent *et al.*, Observation of laser wakefield acceleration of electrons," Phys. Rev. Lett. **81**, 995 (1998).
[6]T. Tajima, X. Yan, and T. Ebisuzaki, "Wakefield acceleration," Rev. Mod. Plasma Phys. **4**, 1–72 (2020).
[7]W. Graves, J. Chen, P. Fromme, M. Holl, R. Kirian, L. Malin, K. Schmidt, J. Spence, M. Underhill, U. Weierstall *et al.*, "Asu compact xfel," in *Proceedings of the 38th International Free-Electron Laser Conference (FEL'17)* (JACoW, 2017).
[8]R. J. England, R. J. Noble, K. Bane, D. H. Dowell, C.-K. Ng, J. E. Spencer, S. Tantawi, Z. Wu, R. L. Byer, E. Peralta *et al.*, "Dielectric laser accelerators," Rev. Mod. Phys. **86**, 1337 (2014).
[9]J. McNeur, M. Kozák, N. Schönenberger, K. J. Leedle, H. Deng, A. Ceballos, H. Hoogland, A. Ruehl, I. Hartl, R. Holzwarth *et al.*, "Elements of a dielectric laser accelerator," Optica **5**, 687–690 (2018).
[10]J. Breuer and P. Hommelhoff, "Laser-based acceleration of nonrelativistic electrons at a dielectric structure," Phys. Rev. Lett. **111**, 134803 (2013).
[11]G. Andonian, "Electron-beam driven dielectric wakefield accelerator experiments in the terahertz regime," AIP Conf. Proc. **1507**, 94–102 (2012).
[12]B. Holzer, "Introduction to particle accelerators and their limitations," arXiv:1705.09601 (2017).
[13]E. I. Simakov, H. L. Andrews, M. J. Herman, K. M. Hubbard, and E. Weis, "Diamond field emitter array cathodes and possibilities of employing additive manufacturing for dielectric laser accelerating structures," AIP Conf. Proc. **1812**, 060010 (2017).
[14]R. J. England, D. Filippetto, G. Torrisi, A. Bacci, G. D. Valle, D. Mascali, G. S. Mauro, G. Sorbello, P. Musumeci, J. Scheuer, B. Cowan, L. Schachter, Y.-C. Huang, U. Niedermayer, W. D. Kimura, R. Li, R. Ishebeck, E. I. Simakov, P. Hommelhoff, and R. L. Byer, "Laser-driven structure-based accelerators," arXiv:2203.08981[physics.acc-ph] (2022).
[15]K. P. Wootton, Z. Wu, B. M. Cowan, A. Hanuka, I. V. Makasyuk, E. A. Peralta, K. Soong, R. L. Byer, and R. J. England, "Demonstration of acceleration of relativistic electrons at a dielectric microstructure using femtosecond laser pulses," Opt. Lett. **41**, 2696–2699 (2016).
[16]L. Liu, X. Ouyang, J. Zhang, X. Zhang, and Y. Zhong, "Polycrystalline CVD diamond detector: Fast response and high sensitivity with large area," AIP Adv. **4**, 017114 (2014).
[17]M. E. Schneider, "Advancing field emission technology for high power injectors operating in GHz and beyond," Ph.D. thesis (Michigan State University, 2022).
[18]J. van der Weide, Z. Zhang, P. Baumann, M. Wensell, J. Bernholc, and R. Nemanich, "Negative-electron-affinity effects on the diamond (100) surface," Phys. Rev. B **50**, 5803 (1994).
[19]M.-A. Pinault, J. Barjon, T. Kociniewski, F. Jomard, and J. Chevallier, "The n-type doping of diamond: Present status and pending questions," Physica B **401**, 51–56 (2007).
[20]U. Mengui, R. Campos, K. Alves, E. Antunes, M. Hamanaka, E. Corat, and M. Baldan, "Combined effect of nitrogen doping and nanosteps on microcrystalline diamond films for improvement of field emission," Appl. Surf. Sci. **334**, 222–226 (2015).
[21]L. Shen and Z. Chen, "An investigation of grain size and nitrogen-doping effects on the mechanical properties of ultrananocrystalline diamond films," Int. J. Solids Struct. **44**, 3379–3392 (2007).
[22]W. Yuan, L. Fang, Z. Feng, Z. Chen, J. Wen, Y. Xiong, and B. Wang, "Highly conductive nitrogen-doped ultrananocrystalline diamond films with enhanced field emission properties: Triethylamine as a new nitrogen source," J. Mater. Chem. C **4**, 4778–4785 (2016).
[23]D. Kim, H. L. Andrews, B. K. Choi, and E. I. Simakov, "Fabrication of micron-scale diamond field emitter arrays for dielectric laser accelerators," in *2018 IEEE Advanced Accelerator Concepts Workshop (AAC)* (IEEE, 2018), pp. 1–3.
[24]D. Kim, H. L. Andrews, B. K. Choi, R. L. Fleming, C.-K. Huang, T. J. Kwan, J. Lewellen, K. Nichols, V. Pavlenko, and E. I. Simakov, "Divergence study and emittance measurements for the electron beam emitted from a diamond pyramid," Nucl. Instrum. Methods Phys. Res. Sect. A **953**, 163055 (2020).
[25]C.-K. Huang, H. L. Andrews, R. C. Baker, R. L. Fleming, D. Kim, T. J. Kwan, A. Piryatinski, V. Pavlenko, and E. I. Simakov, "Modeling of diamond field emitter arrays for a compact source of high brightness electron beams," J. Appl. Phys. **125**, 164501 (2019).
[26]C. Huang, H. Andrews, R. Baker, R. Fleming, D. Kim, T. Kwan, V. Pavlenko, A. Piryatinski, and E. Simakov, "Physics of electron beam generation and dynamics from diamond field emitter arrays," in *Proceedings of 10th International Particle Accelerator Conference* (JACoW, 2019), pp. 2137–2139.
[27]K. Nichols, H. L. Andrews, D. Kim, E. I. Simakov, M. Conde, D. S. Doran, G. Ha, W. Liu, J. Power, J. Shao *et al.*, "Demonstration of transport of a patterned electron beam produced by diamond pyramid cathode in an rf gun," Appl. Phys. Lett. **116**, 023502 (2020).
[28]H. Andrews, K. Nichols, D. Kim, E. I. Simakov, S. Antipov, G. Chen, M. Conde, D. Doran, G. Ha, W. Liu *et al.*, "Shaped beams from diamond field-emitter array cathodes," IEEE Trans. Plasma Sci. **48**, 2671–2675 (2020).
[29]O. Chubenko, S. S. Baturin, and S. V. Baryshev, "Theoretical evaluation of electronic density-of-states and transport effects on field emission from n-type ultrananocrystalline diamond films," J. Appl. Phys. **125**, 205303 (2019).
[30]J. D. Jarvis, H. Andrews, B. Ivanov, C. Stewart, N. De Jonge, E. Heeres, W.-P. Kang, Y.-M. Wong, J. Davidson, and C. Brau, "Resonant tunneling and extreme brightness from diamond field emitters and carbon nanotubes," J. Appl. Phys. **108**, 094322 (2010).
[31]G. Chen, G. Adhikari, L. Spentzouris, K. K. Kovi, S. Antipov, C. Jing, W. Andreas Schroeder, and S. V. Baryshev, "Mean transverse energy of ultrananocrystalline diamond photocathode," Appl. Phys. Lett. **114**, 093103 (2019).
[32]K. J. Pérez Quintero, S. Antipov, A. V. Sumant, C. Jing, and S. V. Baryshev, "High quantum efficiency ultrananocrystalline diamond photocathode for photoinjector applications," Appl. Phys. Lett. **105**, 123103 (2014).
[33]G. Chen, L. Spentzouris, C. Jing, M. Conde, G. Ha, W. Liu, J. Power, E. Wisniewski, A. V. Sumant, S. Antipov *et al.*, "Demonstration of nitrogen-incorporated ultrananocrystalline diamond photocathodes in a rf gun environment," Appl. Phys. Lett. **117**, 171903 (2020).


10 April 2025 23:03:47


© Author(s) 2024

[34]A. Kachwala, O. Chubenko, D. Kim, E. Simakov, and S. Karkare, "Quantum efficiency, photoemission energy spectra, and mean transverse energy of ultrananocrystalline diamond photocathode," J. Appl. Phys. **132**, 224901 (2022).
[35]E. Simakov, H. Andrews, R. Fleming, D. Kim, V. Pavlenko, D. Black, and K. Leedle, "Observations of the femtosecond laser-induced emission from the diamond field emitter tips," in *10th International Particle Accelerator Conference (IPAC'19), Melbourne* (JACoW, 2019).
[36]V. Pavlenko, H. Andrews, D. Gorelov, R. Fleming, D. Kim, E. Simakov, K. Leedle, and D. Black, "Characterization of femtosecond-laser-induced electron emission from diamond nano-tips," in *North American Particle Accelerator Conference (NAPAC'19), Lansing, MI, 01–06 September 2019* (JACOW Publishing, Geneva, 2019), pp. 228–231.
[37]V. Pavlenko, D. Kim, H. L. Andrews, D. V. Gorelov, and E. I. Simakov, "Strong-field photoemission experiment using diamond field emitter arrays," arXiv:2107.00128 (2021).
[38]See https://www.focus-gmbh.com for "FOCUS-IS-IEF-PEEM."
[39]M. Reutzel, A. Li, and H. Petek, "Above-threshold multiphoton photoemission from noble metal surfaces," Phys. Rev. B **101**, 075409 (2020).
[40]M. Krüger, "Attosecond physics in strong-field photoemission from metal nanotips," Ph.D. thesis (LMU, 2013).
[41]F. Giustino, S. G. Louie, and M. L. Cohen, "Electron-phonon renormalization of the direct band gap of diamond," Phys. Rev. Lett. **105**, 265501 (2010).
[42]A. Tafel, S. Meier, J. Ristein, and P. Hommelhoff, "Femtosecond laser-induced electron emission from nanodiamond-coated tungsten needle tips," Phys. Rev. Lett. **123**, 146802 (2019).
[43]L. Keldysh *et al.*, "Ionization in the field of a strong electromagnetic wave," Sov. Phys. JETP **20**, 1307–1314 (1965).
[44]See https://www.ansys.com for "Ansys-Lumerical-FDTD."
[45]M. Ficek, K. J. Sankaran, J. Ryl, R. Bogdanowicz, I.-N. Lin, K. Haenen, and K. Darowicki, "Ellipsometric investigation of nitrogen doped diamond thin films grown in microwave $CH_4/H_2/N_2$ plasma enhanced chemical vapor deposition," Appl. Phys. Lett. **108**, 241906 (2016).
[46]C. Kealhofer, S. M. Foreman, S. Gerlich, and M. A. Kasevich, "Ultrafast laser-triggered emission from hafnium carbide tips," Phys. Rev. B **86**, 035405 (2012).
[47]H. Elsayed-Ali, T. Norris, M. Pessot, and G. Mourou, "Time-resolved observation of electron-phonon relaxation in copper," Phys. Rev. Lett. **58**, 1212 (1987).
[48]W. Fann, R. Storz, H. Tom, and J. Bokor, "Direct measurement of nonequilibrium electron-energy distributions in subpicosecond laser-heated gold films," Phys. Rev. Lett. **68**, 2834 (1992).
[49]M. Bionta, B. Chalopin, A. Masseboeuf, and B. Chatel, "First results on laser-induced field emission from a CNT-based nanotip," Ultramicroscopy **159**, 152–155 (2015).
[50]M. R. Bionta, S. J. Weber, I. Blum, J. Mauchain, B. Chatel, and B. Chalopin, "Wavelength and shape dependent strong-field photoemission from silver nanotips," New J. Phys. **18**, 103010 (2016).
[51]J. Maxson, P. Musumeci, L. Cultrera, S. Karkare, and H. Padmore, "Ultrafast laser pulse heating of metallic photocathodes and its contribution to intrinsic emittance," Nucl. Instrum. Methods Phys. Res. Sect. A **865**, 99–104 (2017).
[52]N. Martin Sabanes, F. Krecinic, T. Kumagai, F. Schulz, M. Wolf, and M. Müller, "Femtosecond thermal and nonthermal hot electron tunneling inside a photoexcited tunnel junction," ACS Nano **16**, 14479–14489 (2022).
[53]J. Che, T. Çağın, W. Deng, and W. A. Goddard III, "Thermal conductivity of diamond and related materials from molecular dynamics simulations," J. Chem. Phys. **113**, 6888–6900 (2000).
[54]S. Tóth, J. Budai, M. Veres, and M. Koós, "Optical properties of nano-and ultrananocrystalline diamond thin layers in the UV and visible spectral range," in *IOP Conference Series: Materials Science and Engineering* (IOP Publishing, 2018), Vol. 426, p. 012049.
[55]R. Rani, K. Panda, N. Kumar, K. A. Titovich, K. V. Ivanovich, S. A. Vyacheslavovich, and I.-N. Lin, "Tribological properties of ultrananocrystalline diamond films: Mechanochemical transformation of sliding interfaces," Sci. Rep. **8**, 283 (2018).
[56]M. Shamsa, S. Ghosh, I. Calizo, V. Ralchenko, A. Popovich, and A. Balandin, "Thermal conductivity of nitrogenated ultrananocrystalline diamond films on silicon," J. Appl. Phys. **103**, 083538 (2008).
[57]J. Huang, Y. Liu, S. Jin, Z. Wang, Y. Qi, J. Zhang, K. Wang, and R. Qiu, "Uniformity control of laser-induced periodic surface structures," Front. Phys. **10**, 932284 (2022).
[58]A. Borowiec and H. Haugen, "Subwavelength ripple formation on the surfaces of compound semiconductors irradiated with femtosecond laser pulses," Appl. Phys. Lett. **82**, 4462–4464 (2003).
[59]J. Bonse, J. Krüger, S. Höhm, and A. Rosenfeld, "Femtosecond laser-induced periodic surface structures," J. Laser Appl. **24**, 042006 (2012).

10 April 2025 23:03:47


© Author(s) 2024